

Formation and Structure of Pachyman Aggregates in Dimethyl Sulfoxide Containing Water

QIONG DING,¹ LINA ZHANG,¹ CHI WU^{2,3}

¹ Department of Chemistry, Wuhan University, Wuhan 430072, People's Republic of China

² Department of Chemistry, The Chinese University of Hong Kong, Shatin, N.T., Hong Kong

³ The Open Laboratory of Bond-Selective Chemistry, Department of Chemical Physics, University of Science and Technology of China, Hefei, Anhui, People's Republic of China

Received 5 January 1999; revised 28 July 1999; accepted 6 August 1999

ABSTRACT: The aggregation of pachyman, β -(1 \rightarrow 3)-D-glucan ($M_w = 1.68 \times 10^5$) from the *Poria cocos* mycelia, was investigated using static and dynamic laser light scattering (LLS) in dimethyl sulfoxide (DMSO) containing about 15% water, which leads to large aggregates. Both the time dependence of hydrodynamic radius and the angle dependence of the scattering intensity were used to calculate the fractal dimension (d_f) of the aggregates. The aggregation rate and average size of aggregates increase dramatically with increasing the polymer concentration from 1.7×10^{-4} g/mL to 8.6×10^{-4} g/mL, and with the decrease of the solvent quality, that is, water content from 13 to 15%. In the cases, the fractal dimensions change from 1.94 to 2.43 and from 1.92 to 2.54, respectively, suggesting that transforms of aggregation processes: a slow process called reaction-limited cluster aggregation (RLCA) to a fast process called diffusion-limited cluster aggregation (DLCA) in different polymer concentrations and water content. The fractal dimensions above 2 of the fast aggregation is larger than the 1.75 predicted for the ideal DLCA model, suggesting that the aggregation involves a restructuring process through the interchain hydrogen bonding interaction. There are no aggregates of pachyman in DMSO without water, but aggregates formed in the DMSO containing 15% water at 25°C as a compact structure. © 1999 John Wiley & Sons, Inc. *J Polym Sci B: Polym Phys* 37: 3201–3207, 1999

Keywords: polysaccharide; pachyman; mycelia; laser light scattering; aggregation; fractal dimension

INTRODUCTION

Aggregation of small particles to form large aggregates is a widespread phenomenon that has attracted much research interest.^{1–6} Polysaccharide, intrinsically involved in human nutrition and, hence, concerned with health, is one of the most important biopolymers.⁷ Because of the

abundance of interchain hydrogen bonds, polysaccharide has a tendency to aggregate. Understanding of the aggregation phenomena of polysaccharides is very important for their application in the food industry and medicine. Recently, the field of aggregation has been the subject of a great amount of studies attributable to the introduction of the mathematical concept of fractal, a rugose object whose rugosities show up at any length scale and the use of simulations on big computers.^{8–13} With this concept of fractal, we can study the kinetics of aggregation, that is, the quantitative description of the time evolution of the mean

Correspondence to: L. Zhang (E-mail: lnzhang@public.wh.hb.cn)

Journal of Polymer Science: Part B: Polymer Physics, Vol. 37, 3201–3207 (1999)
© 1999 John Wiley & Sons, Inc. CCC 0887-6266/99/223201-07

size and their size distribution, and the geometry, that is, the quantitative description of the structure.¹⁰ In the general theory of fractal, the fractal dimension d_f was defined as the dependence of the total mass on the characteristic length scale on which the fractal is examined.^{8–11} Various kinds of computer simulations and phenomenological models are present to elucidate the experimental results. Generally, there are two regimes of aggregation: the fast process called diffusion-limited cluster aggregation (DLCA)—in which every collision between particles results in the formation of a permanent contact, and the slow process, called reaction-limited cluster aggregation (RLCA)—in which only a small fraction of particle collisions leads to the formation of a contact. The former process results in a loose, ramified structure and exhibits power-law kinetic with $R \propto t^{1/d_f}$, where R is the hydrodynamic radius of the cluster and t is the time, with a fractal dimension d_f of 1.75 ± 0.05 in three dimension, while the latter yield a more compact structure and shows exponential kinetics with $R \propto e^{\Gamma t}$, d_f of 2.05 ± 0.05 .¹⁴ However, both DLCA and RLCA models are also limited to certain ideal conditions and irreversible aggregation models, that is, the particle or the cluster, as soon as it sticks, stays rigidly in its sticking position. All possibilities of dissociation and collapse are excluded. In real experiments, restructuring phenomena, accompanied with cluster deformations, are more or less present either during or at the end of the aggregation process.^{10,15,16} It was found that aggregates with an initially lower d_f of 1.75 can restructure to a more compact structure of a higher d_f 2.1¹⁶ or 2.4¹⁷ after a certain time, and then they are completely stable. In principle, at least, this may also be true of those formed during the slow process as well.¹⁶ The DLCA model have been modified by Shih, Aksay, and Kikuchi (SAK), with a finite interparticle bonding energy, which yields aggregates with various fractal dimension ranging from 1.4 to 2.0 in two dimension.¹⁸ Liu et al.¹⁹ studied the aggregation with finite interparticle attraction energies, and showed that the aggregates of colloidal particles can still be fractal objects with a finite interparticle attraction, and the fractal dimension changes from 1.74 to 2.68 with the interparticle attraction energy. These results were in agreement with the computer simulations of SAK. The fast aggregation rates produced a larger value ($d_f > 1.75$) of the fractal dimension in their study. Dynamic laser light scattering to monitor the ag-

gregation indicated that the measured fractal dimensions was found to increase with an increase in the aggregation rate and in the salt concentration, as well as the temperature.²¹

Previously, we have investigated the polysaccharide PC3, a linear β -(1 \rightarrow 3)-D-glucan from the sclerotium of *Poria cocos*, and found the aggregation phenomenon in aqueous solution using dynamic laser light scattering, analytical size-exclusion chromatography (SEC), viscometry, and membrane osmometry under different conditions.^{22–24} These results proved that the polysaccharide formed aggregates in aqueous solution or in dimethyl sulfoxide (DMSO) with LiCl absorbed moisture, and the aggregates can be broken by DMSO without water, cadoxen, or at 80°C. The purpose of this article is to study in detail the kinetics and geometry of polysaccharide aggregates by static and dynamic LLS to elucidate the feature of aggregates using different models. The influence of several factors, including the solvent quality and the polymer concentration on the aggregation, are also studied and discussed.

EXPERIMENTAL

Sample Preparation

The *Poria cocos* mycelia were cultured, and the polysaccharide was extracted in a 0.5 *N* sodium hydroxide (NaOH) aqueous solution. The gas chromatography (GC) and Nuclear Magnetic Resonance (NMR) showed that the polysaccharide consisted of β -(1 \rightarrow 3)-D-glucose residues, and identified as pachyman.²⁵ The fractionation was made by using a SEC column (550 mm \times 20 m) packed with cellulose gel particles prepared in our lab,²⁶ with DMSO as the elute at 25°C. The unfractionated sample and two fractions used in this study are marked as F0, F1, and F2.

Solution Preparation

Dimethyl Sulfoxide (DMSO) (Sigma, A.R.), treated with a molecular sieve to make it devoid of water, was used as the solvent. A relatively concentrated stock solution was prepared by completely dissolving the proper amount of polysaccharide in the solvent. After a complete dissolution, this stock solution was centrifuged at 15,000 rpm for 8 h to remove a trace amount of insoluble substances. A series of solutions with different desired concentrations were obtained by a succes-

sive dilution of such a clarified stock solution. Finally, each solution was further clarified with a 0.1- μm Waterman filter (Anotop), depending on the chain size. Adding water into the polysaccharide–DMSO system induced aggregation. The dynamic LLS was performed 1 min later after the addition of water. Ten to 30 min later after the formation of aggregates, the static LLS of the samples was measured at different angles.

Laser Light Scattering (LLS)

In static LLS, the excess absolute scattered light intensity [also known as Rayleigh ratio, $R_{vv}(\theta)$] of a polymer solution at a relatively low angle (θ) and low concentration (c) is related to the weight-average molar mass (M_w) by²⁷

$$\frac{KC}{R_{vv}(q)} \approx \frac{1}{M_w} \left(1 + \frac{1}{3} \langle R_g^2 \rangle_z q^2 \right) + 2A_2C \quad (1)$$

where $K = 4\pi^2 n^2 (dn/dc)^2 / (N_A \lambda_0^4)$ and $q = (4\pi n / \lambda_0) \sin(\theta/2)$ with N_A , n , and λ_0 being Avogadro's number, the solvent refractive index, and the wavelength of light in the vacuum, respectively; $\langle R_g^2 \rangle_z^{1/2}$ (or written as $\langle R_g \rangle$) is the z -average radius of gyration; and A_2 is the second virial coefficient.

By measuring $R_{vv}(q)$ at different C and q , we can determine M_w , $\langle R_g \rangle$, and A_2 from the Zimm plot.

In dynamic LLS, an intensity–intensity time correlation function $G^{(2)}(t, q)$ in the self-beating mode was measured^{28,29} and

$$G^{(2)}(t, q) = A[1 + \beta |g^{(1)}(t, q)|^2] \quad (2)$$

where A is a measured baseline; β , a parameter, depending on the coherence of the detection; t , the delay time; and $g^{(1)}(t, q)$, the normalized first-order electric field time correlation function. For a polydisperse sample, $g^{(1)}(t, q)$ can be related to the line-width distribution $G(\Gamma)$ by

$$g^{(1)}(t, q) = \int_0^\infty G(\Gamma) e^{-\Gamma t} d\Gamma \quad (3)$$

using the analysis program CONTIN.³⁰ $G(\Gamma)$ can be further reduced to a translational diffusion coefficient distribution $G(D)$ if the relaxation is diffusive.

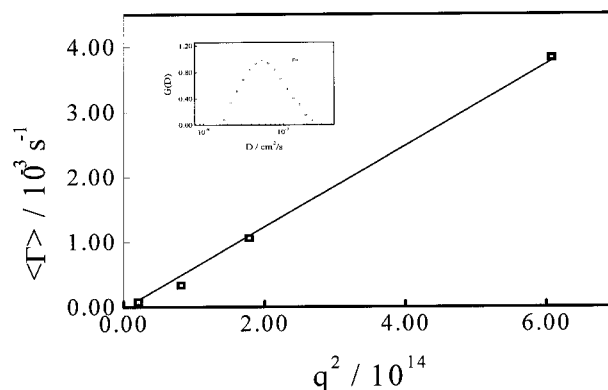


Figure 1. q^2 dependence of $\langle \Gamma \rangle$ for pachyman F0 in DMSO at 25°C, where $c = 1 \times 10^{-3}$ g/mL. The insert shows the translational diffusion coefficient distribution $G(D)$ of the sample.

A commercial LLS spectrometer (ALV/SP-150, Langen in Hessen, Germany) that was equipped with an ALV-5000 multitaup digital time correlator and a 400-MW ADLAS DPY 425 II solid-state laser ($\lambda = 532$ nm) as the light source was used. The primary beam was vertically polarized. All the LLS measurements were performed at $25.0 \pm 0.1^\circ\text{C}$. The specific refractive index increment dn/dc was determined by a novel differential refractometer that was incorporated into the LLS spectrometer,³¹ wherein the same laser light source was used for both the LLS spectrometer and the refractometer, so that the wavelength correction of dn/dc was avoided. The value of dn/dc for the polysaccharide was measured to be $0.0426 \text{ cm}^3/\text{g}$ in DMSO.

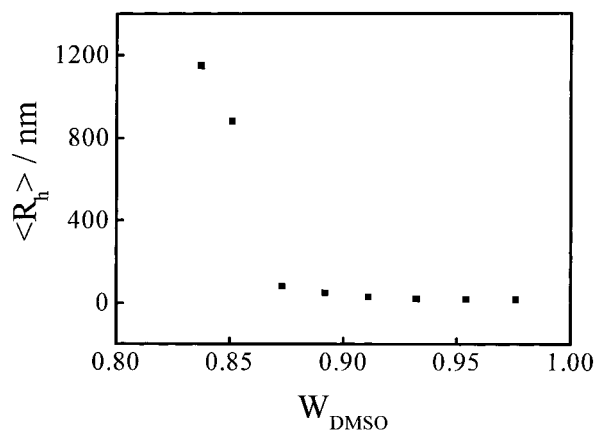
RESULTS AND DISCUSSION

The pachyman from *Poria cocos* mycelia in DMSO was first characterized. Figure 1 shows that the average line width $\langle \Gamma \rangle$ ($\equiv \int_0^\infty G(\Gamma) \Gamma d\Gamma$) is a linear function of q^2 , indicating that the relaxation process measured in dynamic LLS is diffusive. The slope of the line in Figure 1 leads to the average translational diffusion coefficient $\langle D \rangle$, that is $\langle \Gamma \rangle / q^2 = \langle D \rangle$. It is worth noting that in the concentration range used, $\langle D \rangle$ is nearly independent on the polysaccharide concentration. Therefore, $G(\Gamma)$ can be transformed into $G(D)$ by using $\Gamma / q^2 = D$, which is shown in the insert of Figure 1, indicating that the pachyman in DMSO has a unimodal translational diffusion coefficient distribution rather than bimodal distribution caused by

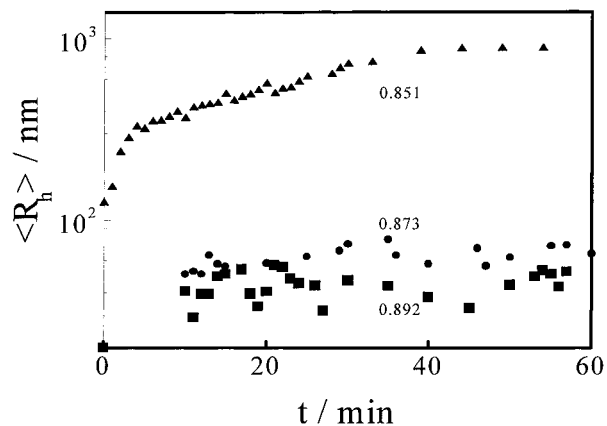
Table I. Summary of Static and Dynamic LLS Results of Three Pachyman Fractions in DMSO at 25°C

Sample	$10^{-5} M_w$ (g/mol)	$10^4 A_2$ (mol · mL/g ²)	$\langle R_g \rangle$ (nm)	$\langle R_h \rangle$ (nm)	$\langle R_g \rangle / \langle R_h \rangle$	$(M_w/M_n)_{\text{cald}}$
F0	1.68	1.82	26.5	15.4	1.7	1.9
F1	3.48	0.76	31.2	16.3	1.9	1.3
F2	2.20	2.35	—	12.3	—	1.5

aggregation.²² Further, the average hydrodynamic radius $\langle R_h \rangle$ is related to $\langle D \rangle$ through the Stokes–Einstein equation: $\langle R_h \rangle = K_B T / (6\pi\eta\langle D \rangle)$. Both the static and dynamic LLS results of the three samples are summarized in Table I. The positive values of A_2 indicate that DMSO is a good solvent for the polysaccharide at 25°C. The M_w decreases in the order of fractionation, which is reasonable. Note that $\langle R_g \rangle / \langle R_h \rangle$ depends on the chain conformation and polydispersity, but not on the chain length,³² for example, $\langle R_g \rangle / \langle R_h \rangle \sim 1.5$ for a flexible chain in a good solvent. In Table I, the values of $\langle R_g \rangle / \langle R_h \rangle$ larger than 1.5 imply that pachyman acts as expanded coil chains in DMSO, consisting with our recent results.³³ Combination of static and dynamic LLS results,^{22,34} that is, M_w and $G(D)$, enable us to estimate the molecular mass distribution of pachyman from its corresponding $G(D)$, which is also summarized in Table I. The polydispersity (M_w/M_n) of the fraction F1 and F2 was lower than that of unfractionated F0, suggesting that the fractionation in DMSO without water by preparation SEC was effective in avoiding aggregation of pachyman. Hence, there is not aggregation in the system of pachyman–DMSO without water.

**Figure 2.** Average hydrodynamic radius R_h of pachyman F0 aggregates after equilibrium as a function of W_{DMSO} at 25°C.

To induce aggregation, water was added into the polysaccharide–DMSO system, changing the solvent quality from good solvent to poor solvent. The average hydrodynamic radius R_h of pachyman aggregates when reaching the equilibrium as a function of W_{DMSO} (DMSO weight fraction in DMSO–water mixture) at 25°C is shown in Figure 2. The average size keeps almost stable from 0.97 to 0.87 until W_{DMSO} reaches 0.85, then increases dramatically with the decrease of W_{DMSO} , showing aggregates grew. We choose the W_{DMSO} range near 0.85 (crucial point). Figure 3 shows the time dependence of the average hydrodynamic radius R_h of pachyman after the addition of water measured at different W_{DMSO} s at 25°C. In all cases of aggregation, the data exhibit considerable scatter as the size increase. These results come from the relatively large size and small number of aggregates actually sampled by the experiment during the short time that data collected for each point. However, despite the scatter, the trend in the data is clear. Weitz et al.,³⁵ also has shown different shapes of the R_h versus t curve. Here, the aggregation rate and the average size of aggregates are found to be very sensi-

**Figure 3.** Time dependence of average hydrodynamic radius R_h of pachyman F0 at different W_{DMSO} (the weight fraction of DMSO in the DMSO–water mixture) at 25°C.

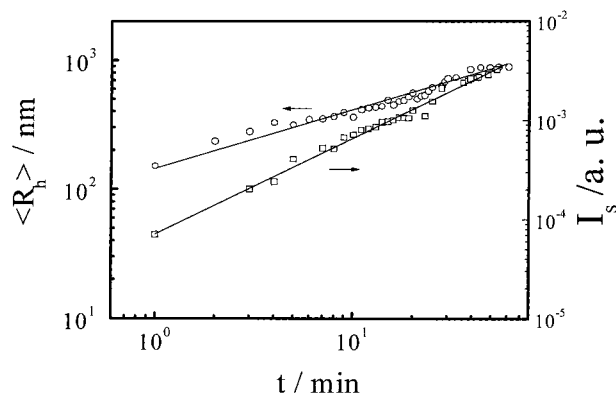


Figure 4. Double-logarithmic plots of R_h and I_s versus t of pachyman F0 at $W_{\text{DMSO}} = 0.851$ at 25°C .

tive to the change of W_{DMSO} , and show different dynamic processes. When W_{DMSO} is in the range of 0.89 to 0.87, the average size changes slightly, which means only a very small amounts of aggregates are formed, that is, slow aggregation (RLCA) occurs, while when W_{DMSO} is about 0.85, fast aggregation turns up. The average size increases dramatically, reaches 800 nm in 60 min, which allows us to monitor the kinetics of aggregation. The slope of the R_h versus t curve decreases with an increase in time, which is the behavior of cluster growth in the diffusion–time-limited regime. In such a regime the R_h exhibits simple power-law dependence on t : $R_h \propto t^{1/d_f}$, where t is the time and d_f is the fractal dimension. The straight line of double-logarithmic plots shown in Figure 4 implies that the power-law growth kinetics are applicable. The values of fractal dimension d_f obtained are summarized in Table II.

Teixeria et al.³⁶ provided another method to calculate the fractal dimension from the static

Table II. The Fractal Dimension d_f of Different Aggregation Process at Different W_{DMSO} , Different Polymer Concentrations, c

W_{DMSO}	c ($\times 10^{-4}$ g/mL)	T ($^\circ\text{C}$)	d_f
0.892	6.8	25	1.92
0.873	6.8	25	2.01
0.851	6.8	25	2.04
0.837	6.8	25	2.54
0.851	1.7	25	1.94
0.851	5.1	25	1.98
0.851	6.8	25	2.04
0.851	8.6	25	2.43

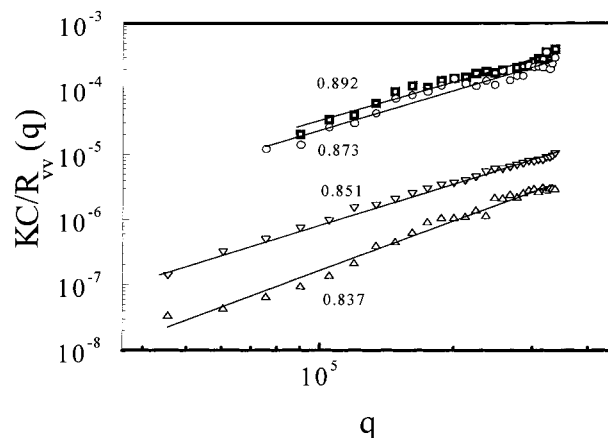


Figure 5. Double-logarithmic plots of $KC/R_{vv}(q)$ versus q of pachyman F0 at different W_{DMSO} s at 25°C .

LLS experiments. For fractal aggregates, the scattering intensity of a given q is related to the fractal dimension d_f in the form: $I(q) \propto q^{-d_f}$ over the range $R_g^{-1} < q < a^{-1}$, where a is the radius of the particle, and R_g is the average radius of gyration of the aggregates. Based on the definition of R_{vv} , there is the relation: $KC/R_{vv}(q) \propto I(q)^{-1}$, so $KC/R_{vv}(q)$ is related to q by: $KC/R_{vv}(q) \propto q^{d_f}$. Thus, the fractal dimension of aggregation can be obtained by the double-logarithmic plot $KC/R_{vv}(q)$ versus q , whose slope in the power-law region gives the fractal dimension d_f . Data for $\log KC/R_{vv}(q)$ versus $\log q$ for different aggregations are present in Figure 5, and the values are also summarized in Table II. The values of the fast aggregation are in good agreement with that from the R_h versus t curve. It indicates that the fractal dimension increases with the decrease of W_{DMSO} and the increase of the aggregation rate. Although the fractal dimensions (1.9–2.0) of the slow aggregation are in agreement with the predict value of 2.05 ± 0.05 , the fractal dimensions above 2.0 of the fast aggregation are apparently larger than the predict values of 1.75 ± 0.05 in the ordinary DLCA model, suggesting that the polysaccharide aggregates have a compact rather than ramified structure. This is similar to the results reported in the literature,^{16–21} attributed to the interparticle interchain energy. Because the polysaccharide contains a large amount of hydroxyl groups, the hydrogen-bonding interaction is much larger than the van der Waals attraction, so it plays an important role in aggregation. In such a case, the growth of the fractal aggregation is divided into two successive mechanistic steps: (1) a kinetic step for the diffusional

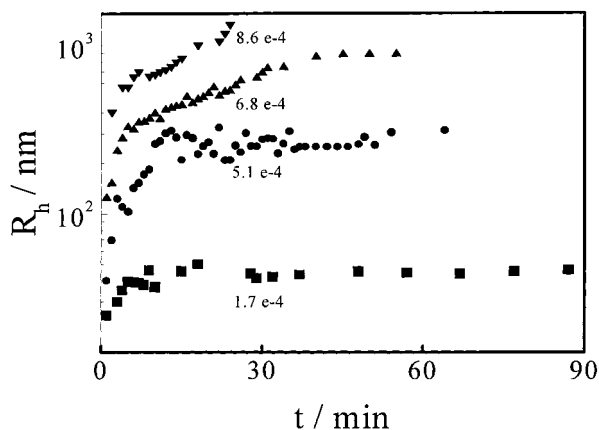


Figure 6. Time dependence of average hydrodynamic radius R_h of pachyman F0 at different polymer concentrations at 25°C.

approach of particle or aggregates, so as to be able to undergo collision; and (2) a subsequent step to allow the aggregates so formed to pack more closely once they come into contact, that is, a restructuring process. The aggregation rate and the fractal dimensions increase with the decrease of solvent quality, that is, the increase of water, because the addition of a relatively weak polar solvent (water) to a strong polar solvent weakens the solvation of solvent (DMSO) and solute, and allows the interchain hydrogen bonding interactions of the solute to be more active, resulting in the restructuring process of aggregation to form a more compact structure and larger fractal dimension.

Figure 6 is the time dependence of average hydrodynamic radius after the addition of water with fixed $W_{\text{DMSO}} = 0.85$ at different polymer concentrations at 25°C. From the data shown in Figure 6 it can be seen that polymer concentrations also affect the aggregation rate and average size of aggregates remarkably. With the increase of polymer concentrations, the aggregation rate and the average size increase. When concentration is 1.7×10^{-4} g/mL, the average size of pachyman in DMSO containing 15% water stays almost stable. From the data shown in Figure 6 it can be seen that when the concentration reaches 8.6×10^{-4} the average size changes dramatically from 40 (for $C = 1.7 \times 10^{-4}$ g/mL) to 1200 nm in 30 min. As mentioned above, a double-logarithmic plot of R_h versus t is used to calculate the fractal dimension (d_f) of fast aggregation, and $KC/R_{vv}(q)$ versus q for the all aggregation shown in Figures 7 and 8, and the d_f results are summarized in

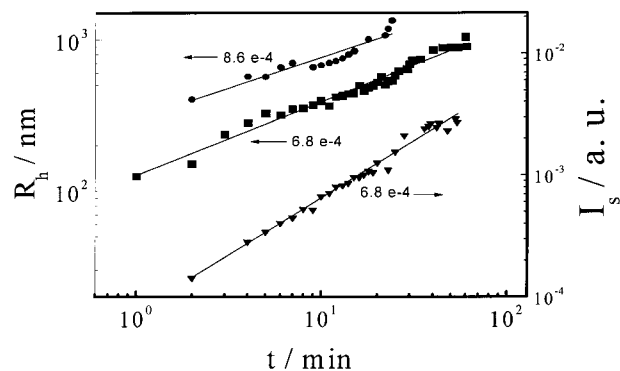


Figure 7. Double-logarithmic plots of R_h and I_s versus t of pachyman F0 at different polymer concentrations at 25°C.

Table II. The fractal dimension increases with the increase of the polymer concentration. The values of d_f of fast aggregation are above 2, in the same range with the values for different W_{DMSO} , further confirming that the aggregation involves a restructuring process.

CONCLUSION

Molecular mass (M_w) of pachyman from *Poria cocos* mycelia is determined by static LLS to be 1.68×10^5 , which is larger than that from *Poria cocos* sclerotium. There are no aggregates of pachyman in DMSO without water, but in DMSO containing 15% water they form aggregates. There are different aggregation processes: a fast one and a slow one, at different solvent quality

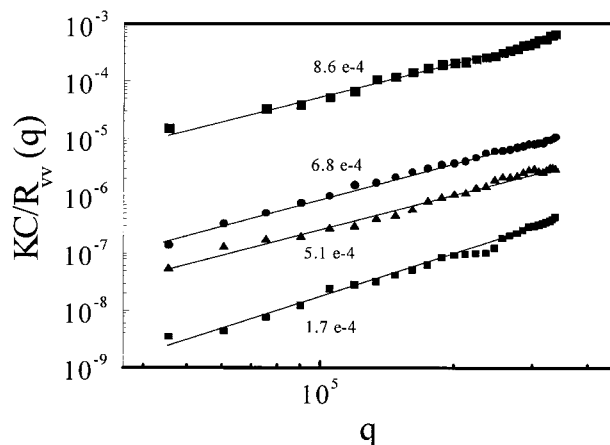


Figure 8. Double-logarithmic plots of $KC/R_{vv}(q)$ versus q of pachyman F0 at different polymer concentrations at 25°C.

and polymer concentrations. The aggregation rate and average size of aggregates of pachyman in DMSO containing 10–16% water increase dramatically with increasing the water content or polymer concentration. The fractal dimension of the fast aggregation is larger than predicted from ideal diffusion-limited cluster aggregation (DCLA), suggesting that the aggregation involved a restructure, and the interchain hydrogen bonding interaction of pachyman in the solution plays an important role in the restructuring process.

The financial support of this work by the National Natural Science Foundation of China (29374170), RGC (the Research Grants Council of the Hong Kong Government) Earmarked Grant 1995/96 (CUHK 299/94P, 221600260), and National Distinguished Young Investigator Fund is gratefully acknowledged.

REFERENCES AND NOTES

1. Chu, E. Y.; Xu, Z. S.; Lee, C. M.; Sek, C. K. F.; Okamoto, Y.; Pearce, E. M.; Kei, F. K. *J Polym Sci Part B Polym Phys* 1995, 33, 71.
2. Vaganova, E.; Yitzchaik, S. *Polym Prepr* 1998, 39, 109.
3. Jenekhe, S. A.; Chen, L. X. *Science* 1998, 279, 1903.
4. Wang, S.; Brisse, F. *Macromolecules* 1998, 31, 2265.
5. Yamamoto, T.; Komarudin, D.; Kubota, K.; Sasaki, S. *Chem Lett* 1998, 3, 235.
6. Yamamoto, T.; Komarudin, D.; Maruyama, T.; Arai, M.; Lee, B. L.; Saganuma, H.; Asakawa, N.; Inoue, Y.; Kubota, K.; Sasaki, S.; Fukuda, T.; Matsuda, H. *J Am Chem Soc* 1998, 120, 2047.
7. Stephen, A. M. *Food Polysaccharide and Their Applications*; Marcel Dekker: New York, 1995.
8. Family, F.; Landau, D. P. *Kinetics of Aggregation and Gelation*; North-Holland: Amsterdam, 1984.
9. Stanley, H. E.; Ostrowsky, N. *On the Growth and Form*; Nijhoff: Dordrecht, 1986.
10. Jullien, R.; Botet, R. *Aggregation and Fractal Aggregates*; World Scientific: Singapore, 1987.
11. Viscek, T. *Fractal Growth Phenomena*; World Scientific: Singapore, 1989.
12. Aharony, A.; Heder, J. *Fractals in Physics*; North-Holland: Amsterdam, 1989.
13. Witten, T.; Sander, L. *Phys Rev Lett* 1981, 47, 1400.
14. Weitz, D. A.; Huang, J. S.; Lin, M. Y.; Sung, J. *Phys Rev Lett* 1985, 54, 46.
15. Onada, G. Y. *Phys Rev Lett* 1985, 45, 226.
16. Aubert, C.; Cannell, D. S. *Phys Rev Lett* 1986, 56, 738.
17. Dimon, P.; Sinbar, S. K.; Weitz, D. A.; Safinaya, C. R.; Smith, G. S.; Varady, W. A.; Lindsay, H. M. *Phys Rev Lett* 1986, 57, 595.
18. Shih, W. Y.; Aksay, I. A.; Kikuchi, R. *Phys Rev A* 1987, 36, 5015.
19. Liu, J.; Shih, W. Y.; Sarikaya, M.; Aksay, I. A. *Phys Rev A* 1990, 41, 3206.
20. Zhou, Z.; Wu, P.; Chu, B. *J Colloid Interface Sci* 1991, 146, 541.
21. Wu, W.; Napper, D. H. *Phys Rev E* 1994, 50, 1360.
22. Ding, Q.; Jiang, S.; Zhang, L.; Wu, C. *Carbohydr Res* 1998, 308, 339.
23. Zhang, L.; Ding, Q.; Zhang, P.; Zhu, R.; Zhou, Y. *Carbohydr Res* 1997, 303, 193.
24. Zhang, L.; Ding, Q.; Meng, D.; Ren, L.; Yang, G.; Liu, Y. *J Chromatogr A* 1999, 839, 49.
25. Ding, Q.; Zhang, L.; Cheung, P. C. K. *Acta Polym Sinica*, to appear.
26. Zhang, L.; Zhou, J.; Yang, G.; Chen, J. *J Chromatogr A* 1998, 816, 131.
27. Zimm, B. *J Chem Phys* 1948, 16, 1093.
28. Pecora, R. *Dynamic Light Scattering*; Plenum Press: New York, 1976.
29. Chu, B. *Laser Light Scattering*; Academic Press: New York, 1974.
30. Bryce, T. A.; Clark, A. H.; Rees, D. A.; Reid, D. S. *Eur J Biochem* 1982, 122, 63.
31. Wu, C.; Xia, K. *Rev Sci Instrum* 1993, 65, 587.
32. Kirkwood, J. G.; Riseman, J. *J Chem Phys* 1948, 16, 565.
33. Ding, Q.; Zhang, L.; Wu, C. *Biopolymers*, submitted.
34. Wu, C. *Macromolecules* 1993, 26, 3821.
35. Weitz, D. A.; Huang, J. S. *Kinetics of Aggregation and Gelation*; North-Holland: Amsterdam, 1984.
36. Teixeira, J. *On the Growth and Form*; Nijhoff: Dordrecht, 1986.